



1 **The Contributions to the Explosive Growth of PM_{2.5} Mass due**
2 **to Aerosols-Radiation Feedback and Further Decrease in**
3 **Turbulent Diffusion during a Red-alert Heavy Haze in**
4 **JING-JIN-JI in China**

5 Hong Wang^{1,2*}, Xiaoye Zhang^{1,3*}, Yao Peng^{1,2}, Hongli Liu¹, Meng Zhang⁴, Huizheng
6 Che¹

7 ¹ State Key Laboratory of Severe Weather (LASW), Chinese Academy of Meteorological Sciences (CAMS), CMA, Beijing 100081, China

8 ² Collaborative Innovation Center on Forecast and Evaluation of Meteorological Disasters, Nanjing University of Information Science & Technology, Nanjing
9 210044, China

10 ³ Center for Excellence in Regional Atmospheric Environment, Institute of Urban Environment, Chinese Academy of Sciences (CAS), Xiamen 361021, China

11 ⁴ Beijing Meteorological Bureau, Beijing 100089, China

12 Correspondence to: Hong Wang (wangh@cma.gov.cn) · Xiaoye Zhang (xiaoye@cma.gov.cn)

13
14

15 **Abstract.** The explosive growth (EG) of PM_{2.5} mass usually resulted in PM_{2.5} extreme levels and severe
16 haze pollution in east China and they were generally underestimated by current atmospheric chemical
17 models. Based on the atmospheric chemical model GRPAES_CUACE, three experiments of background
18 (EXP_bk), normal turbulent diffusion and aerosols feedback (EXP_td_af), and retaining 20% of normal
19 turbulent diffusion of chemical tracers of EXP_td_af (EXP_td20_af) are designed to study the contributions
20 to the EG of PM_{2.5} due to aerosols-radiation feedback (AF) and further decrease in turbulent diffusion
21 (DTD) focusing on a red-alert heavy haze in JING-JIN-JI of China. The study results showed that turbulent
22 diffusion coefficient (DC) calculated by EXP_bk is about 60-70m²/s on clear day and 30-35m²/s on haze
23 day. This difference of DC was not enough to discriminate the unstable atmosphere on clear day and
24 extreme stable atmosphere during EG stage of PM_{2.5}, and the inversion calculated by EXP_bk was
25 obviously weaker than the actual atmosphere of sounding observation on haze day. This led to 40-51%
26 underestimation of PM_{2.5} EG by EXP_bk; AF reduced about 43-57% of DC during EG stage of PM_{2.5},
27 which strengthened the local inversion obviously on haze day and local inversion by EXP_td_af was much



28 closer to the sounding observation than that by EXP_bk. This resulted in 20-25% reduction of model errors
29 of $PM_{2.5}$ and it was as low as -16 to -11%. However, the inversion by EXP_td_af was still weaker than the
30 actual observation and AF could not solve all the problems of $PM_{2.5}$ underestimation. Based on EXP_td_af,
31 80% DTD of chemical tracers resulted in a near-zero turbulent diffusion named as “turbulent intermittent ”
32 atmosphere state in EXP_td20_af resulting in a further 14-20% reduction of $PM_{2.5}$ underestimation and the
33 negative $PM_{2.5}$ errors of was reduced to -11 to 2% during the EG stage of $PM_{2.5}$. The combined effects of
34 AF and DTD solved over 79% underestimation of $PM_{2.5}$ EG in this case study. The results showed that the
35 online calculation of aerosol-radiation feedback and a further improving arithmetic of PBL scheme
36 focusing on extreme stable atmosphere stratification are indispensable for reasonable description of local
37 “turbulent intermittent” and more accurate prediction of $PM_{2.5}$ EG and high levels during the severe haze in
38 Jing-Jin-Ji in China.

39 **Keywords:** Aerosols-Radiation Feedback; Turbulent Diffusion; PBL Scheme; Temperature Inversion;
40 $PM_{2.5}$



41 **1 Introduction**

42 East China experienced unprecedented intrusions of severe hazes accompanied by high level of
43 particulate matter less than 2.5 micron in aerodynamic diameter ($PM_{2.5}$) caused wide public concern since
44 2013 until now (Ding et al., 2013; Wang et al. 2013; Huang et al., 2014; Wang et al., 2014; Sun et al., 2014;
45 Hua et al., 2015; Yang et al., 2015; Yang et al., 2016; Zhong et al., 2017, 2018). Instant $PM_{2.5}$ concentration
46 usually reached hundreds, or even one thousand $\mu g/m^3$ occasionally, in the metropolitans in Beijing (JING),
47 Tianjin (JIN), Hebei province (alias JI) and their near surroundings of East Shanxi, West Shandong, and
48 North Henan in east China (abbreviated this region as JING-JIN-JI in this study) during severe haze
49 episodes (Wang et al., 2014; Quan et al., 2014; Sun et al., 2014; Yang et al., 2015; Zheng et al., 2016).
50 Studies showed that models generally underestimated the explosive growth (EG) and peak values of $PM_{2.5}$
51 during the severe hazes in Jing-Jin-Ji in China (Wang et al., 2013; Wang et al., 2014; Li et al., 2016).

52 The causes of $PM_{2.5}$ EG and its underestimation by atmosphere chemical models are complex and
53 uncertain at present, which may involve in local emission, regional transportation, aerosol physicochemical
54 processes, gases-particles conversion, meteorology condition, and so on. However, the actual atmospheric
55 stability and how accurate it is described by atmospheric models is a fundamental problem that can't be
56 ignored among others. Local or regional meteorology condition dictates whether the haze occurs and what
57 the $PM_{2.5}$ level may be (Zhang et al., 2013; Zheng et al., 2015; Gao et al., 2016) when source emissions are
58 unchanged for a short period of time. The meteorology condition of planetary boundary layer (PBL) is the
59 key and direct trigger for touching off a haze event (Wang et al., 2014; Li et al., 2016; Zhong et al., 2017).
60 Turbulent diffusion is an important factor to characterize PBL meteorology when the atmosphere is stable.
61 It is also the major way of particles and gas pollutants exchanging from surface to upper atmosphere and
62 further cleaned by the upper winds when haze occurs accompanied by calm surface wind and weak vertical
63 motion of air in surface and PBL. The intensity of turbulent diffusion largely determines the severity of
64 haze pollution. Reasonable description of turbulent diffusion by PBL schemes in atmospheric chemical
65 models is determinant for severe pollution prediction (Hong et al., 2006; Wang et al., 2015; Hu et al., 2012,
66 2013a, 2013b; Li et al., 2016). The latest studies showed (Wang et al., 2015; Li et al., 2016) that current
67 PBL schemes may be insufficient enough for describing the extreme weak turbulent diffusion condition
68 when extremely severe hazes occurred in JING-JIN-JI, which may be one important reason for the



69 underestimating of $PM_{2.5}$ peaks by model. There may be two independent reasons resulting in this
70 deficiency description of extreme weak turbulent diffusion in atmospheric models. One is that aerosols
71 radiation feedback (AF) is not calculated online in the model run. AF can restrain turbulence by cooling
72 surface and PBL while heating the atmosphere above it (Wang et al., 2010; Forkel et al., 2012; Gao et al.,
73 2014, 2015; Wang et al., 2015; Ding et al., 2016; Li et al., 2016; Miao et al., 2106; Petaja et al., 2016; Gao
74 et al., 2017; Qiu et al., 2017; Zhong et al., 2018). Ignoring AF is likely to lead to obvious overestimation of
75 turbulent diffusion when $PM_{2.5}$ exceeds certain value, which is worthy of further study. Another possible
76 reason is that the extreme weak turbulence resulting to extremely severe hazes is not fully described by the
77 atmospheric chemical model (Li et al., 2016). A Red-alert Heavy Haze occurred on 15 to 17 December,
78 2016 in JING-JIN-JI in China was elected to study the contributions to $PM_{2.5}$ EG and peaks during severe
79 haze due to AF and the possible deficiency in description of the extreme weak turbulent diffusion of
80 atmosphere models in this study.

81 **2 Model, Data and Methodology**

82 **2.1 GRAPES_CUACE Model**

83 The double way atmospheric chemical model GRAPES_CUACE was established focusing on
84 simulation and prediction of dust and haze pollutions in China and East Asia. Trans-city and regional
85 transportation of $PM_{2.5}$, aerosols-radiation-PBL-meteorology interactions, and aerosols-cloud interactions
86 etc. had been widely simulated and studied by using it (Wang et al., 2009, 2010, 2015a, 2015b; Zhou et al.,
87 2012, 2016; Jiang et al., 2015; Zhang et al., 2018). GRAPES_CUACE is also used in this study.
88 Considering interregional transport of gas and particle pollutants in the main polluted areas in eastern China,
89 the model domain includes the whole east China (100-140°E, 20-60°N) (figure 1a), but our study mainly
90 focuses on Jing-Jin-Ji region (the red box in figure 1a). Figure 1b shows the detailed geographical location
91 and topography of JING-Jin-Ji. The black dots in Figure 1a are the locations of $PM_{2.5}$ observation stations.
92 The model horizontal resolution is adopted as $0.15^\circ \times 0.15^\circ$ to match the resolution of emission source data
93 used in this study. There are two balloon sounding stations, Xingtai and Beijing (Figure 1b) in our study
94 area. Xingtai, located in southern Hebei province, the eastern foot of Taihang Mountains and it is
95 influenced by the sinking airflow from Taihang Mountains in winter, is the most polluted city and the $PM_{2.5}$



96 concentrations usually ranked the first in China in recently years. The topography of Xingtai and the
97 serious haze pollution closely related to it are the typical representative of the southern plain of Jing-Jin-Ji.
98 Beijing lies in the transitional zone from Yan Mountain to its southern plain, next to Tianjin and surrounded
99 by Hebei, representing the polluted areas in the central part of Jing-Jin-Ji.

100 2.2 Emission Inventory

101 5 kinds of emission sources of industrial, human life, agricultural, natural and traffic are obtained by
102 the data statistics of China national industry factories, energy consumption, road net and motor vehicles,
103 population information, land use, vegetation cover and etc. in 2015. The 32 kinds of monthly gridded
104 emission inventories of $0.15^{\circ} \times 0.15^{\circ}$ horizontal resolution required by GRAPES_CUACE model, including
105 5 reactive gases, i.e. SO_2 , NO , NO_2 , CO , NH_3 , 20 VOCs, i.e. ALD, CH_4 , CSL, ETH, HC_3 , HC_5 , HC_8 ,
106 HCHO, ISOP, KET, NR, OL_2 , OLE, OLI, OLT, ORA_2 , PAR, TERPB, TOL, XYL and 5 aerosols species, i.e.
107 black carbon, organic carbon, sulfate, nitrate and fugitive dust, are based on above five emission sources
108 according to the emission mode and VOCs partition scheme by CAO (Cao et al., 2016, 2010).

109 2.3 Data Used

110 Hourly averaged observation $\text{PM}_{2.5}$ data for more than 1440 surface observational stations from China
111 National Environmental Monitoring Centre (CNEMC) (<http://www.cnemc.cn>) from 15 to 23 December
112 2016 were used to evaluate the model results. The meteorological balloon sounding data at 00UTC (early
113 morning) and 12UTC (and dusk in local time) in Xingtai and Beijing from China Meteorology
114 Administration (CMA) during the same period were also used compare with the modeled results. NCEP
115 $0.25^{\circ} \times 0.25^{\circ}$ global analysis grids data (<https://rda.ucar.edu/datasets/ds083.3>) were used as the model initial
116 and every 6-hour lateral boundary meteorology input fields. The initial values of chemical tracers were
117 obtained according to the five-year mean climatic values. The results of the first 120 hours of model start
118 are split out to eliminate the effects of chemical initial fields.

119 2.4 Experiments Design

120 Three experiments of EXP_bk, EXP_td_af, and EXP_td20_af were designed to discuss the relative
121 contributions to $\text{PM}_{2.5}$ EG due to AF and a further 80% decrease in turbulent diffusion (DTD) of chemical
122 tracers based on EXP_td_af representing a compensation for the insufficient description of extremely weak



123 turbulent diffusion by PBL scheme in atmospheric chemical model (the detailed descriptions of the
124 experiments listed in Table 1). All other model dynamic process, physical options and initial input data of
125 meteorology and chemical tracers are same for the three experiments except for the differences shown in
126 Table 1.

127 3 Results and Discussions

128 This haze episode began on 15 December, 2016. $PM_{2.5}$ began to gather and climb slowly from 15 to
129 16, but were below $150 \mu\text{g}/\text{m}^3$ in most JING-Jin-Ji region and we name this period as the climbing stage
130 (CS) of $PM_{2.5}$; From 17 to 20 December, $PM_{2.5}$ increased sharply and most of the study area reached the
131 $PM_{2.5}$ peaks of $400\text{--}600 \mu\text{g}/\text{m}^3$ rapidly during this period, which is named as the explosive growth (EG)
132 stage (EGS) of $PM_{2.5}$. This section mainly focuses on the contributions to the $PM_{2.5}$ EG due to AF and
133 further DTD.

134 3.1 The Comparison study of observation and three experiments

135 Figure 2 displays the averaged observed $PM_{2.5}$ ($PM_{2.5_OBS}$) and simulated $PM_{2.5}$ of Exp_bk
136 ($PM_{2.5_bk}$), EXP_td_af ($PM_{2.5_td_af}$) and EXP_td20_tf ($PM_{2.5_td20_af}$) experiments during EGS. It can be
137 seen from $PM_{2.5_OBS}$ that the averaged $PM_{2.5}$ values were generally over $100 \mu\text{g}/\text{m}^3$ in east China and
138 JING-JIN-JI covered the most polluted areas and $PM_{2.5}$ reached up to 300 to $400 \mu\text{g}/\text{m}^3$ in parts of Beijing,
139 Tianjin, Middle-south Hebei province, western frontier region of Shandong province and north Henan
140 province. The $PM_{2.5}$ center of $500\text{--}700 \mu\text{g}/\text{m}^3$ appeared in south Hebei and North Henan province and the
141 $PM_{2.5}$ maximum of $700 \mu\text{g}/\text{m}^3$ was found in south Hebei. The comparison study of $PM_{2.5_bk}$ and
142 $PM_{2.5_OBS}$ shows that $PM_{2.5_bk}$ is obvious lower than $PM_{2.5_OBS}$ on the whole. It is noteworthy that
143 EXP_bk fail to simulate the $PM_{2.5}$ over $300 \mu\text{g}/\text{m}^3$. $PM_{2.5_OBS}$ is about 200 to $300 \mu\text{g}/\text{m}^3$ over most
144 Shandong province while the $PM_{2.5_bk}$ is only 100 to $200 \mu\text{g}/\text{m}^3$ in this region. Compared with $PM_{2.5_bk}$,
145 $PM_{2.5_td_af}$ values are significantly improved by AF and they are much closer to the $PM_{2.5_OBS}$. High
146 $PM_{2.5_OBS}$ centers of 300 to 400 , 400 to 500 , 500 to $600 \mu\text{g}/\text{m}^3$ are almost simulated by EXP_td_af,
147 indicating the important effects of AF on the model simulation of $PM_{2.5}$ high values. However, the areas of
148 the simulated $PM_{2.5}$ values of 300 to 400 , 400 to 500 , 500 to $600 \mu\text{g}/\text{m}^3$ are still smaller than that of the
149 $PM_{2.5_OBS}$. EXP_td_af also fails to simulate the maximum $PM_{2.5}$ values over $600 \mu\text{g}/\text{m}^3$ observed in south



150 Hebei province. $PM_{2.5_td20_af}$ just makes up for this shortage, comparing with $PM_{2.5_bk}$ and $PM_{2.5_td_af}$,
151 $PM_{2.5_td20_af}$ is undoubtedly the closest to $PM_{2.5_OBS}$ both in $PM_{2.5}$ extreme and its influence area. This
152 study result illustrates that both AF and DTD in atmospheric chemical models are required for the effective
153 prediction of $PM_{2.5}$ EG during the severe haze in JING-JIN-JI in China.

154 3.2 The aerosols reform on local atmosphere temperature profiles

155 Some studies offline and online indicated the reforming of atmosphere temperature profile due to
156 aerosols direct radiation (Wang et al., 2010, 2015b; Forkel et al., 2012; Gao et al., 2014, 2015; Wang et al.,
157 2014; Gao et al., 2016; Ding et al., 2016). In our previous works (Wang et al., 2015a, 2015b), AF of
158 composite aerosols from black carbon, organic carbon, sulfate, nitrate, dust, ammonium, and sea salt
159 aerosols had been online coupled into the in GRAPES_CAUCE model. On this basis, the changes of mean
160 temperature profile of Jing-Jin-Ji region of daytime due to aerosols radiation were calculated from 15 to 20
161 December, 2016 in this work. It can be seen from Figure 3 that AF cooled the atmosphere below 750 to 800
162 hPa while warmed the atmosphere above this height. Considering planetary boundary Layer (PBL) height
163 may be as low as several hundreds to one thousand meters when severe hazes occurs in Jing-Jin-Ji (Wang et
164 al., 2015a, Zhong et al., 2017), it may be concluded that whole PBL and its near upper atmosphere was
165 cooled by AF to a different extent during the different stage of this haze. The aerosols' warming effects
166 above 750-850hPa height were very weak and the temperature changes among different days were also
167 small. However, the aerosols' cooling effects shows the most differences from surface to 975 hPa height on
168 different day. The surface daytime cooling is about 2.2 K on 19, 1.5K on 18 and 20, 1K on 17, and 0.5-0.6
169 K on 15 to 16 December. This aerosols' cooling effect decreased rapidly with the height. The difference of
170 cooling rates between surface and 850hPa is 1.8 K on 19, 1.3K on 18 and 20, 1K on 17, and 0.3-0.4 K on
171 15 and 16 December. It can be seen that the AF cooling difference between surface and upper PBL during
172 EGS are much bigger than those during CS. Such obvious difference of cooling effect on surface to upper
173 PBL due to AF may result in the further intensification of the temperature inversion layer pre-existed
174 during the haze event.

175 The vertical sounding meteorology data in Beijing and Xingtai in JING-JIN-JI can be used to prove if
176 this change of the temperature profile by AF is correct. Figure 4 shows the vertical temperature profiles of



177 sounding observation and the modeled temperature profiles of EXP_bk and EXP_td_af during CS (Figure
178 4a) and EGS (Figure 4b) at the two stations. The temperature profiles (Figure 4a) shows that both modeled
179 results by EXP_bk and EXP_td_af partly simulated the observed temperature inversion in Beijing and
180 Xingtai on 15 to 16. The very little difference between the temperature profiles of EXP_bk and EXP_td_af
181 indicated that aerosols radiation had very little impacts on the temperature profiles and local inversion
182 during CS. Nevertheless, Figure 4b shows that the observed temperature inversions were obvious stronger
183 and the inversion depth thicker on 18 to 19 (during EGS of PM_{2.5}) than those on 15 to 16 Dec (CS of PM_{2.5})
184 both in Xingtai and Beijing. The temperate profiles by EXP_td_af were much closer to the observation
185 results than that by EXP_bk, and especially, the temperature inversions were much stronger and also closer
186 to the observation than that by EXP_bk. This result proved the effective correction of local inversions by
187 AF during the EGS of PM_{2.5}. However, it also can be seen, that the inversions by EXP_td_af, which
188 included online AF, are still weaker than the truth observed inversion in the two stations, suggesting that
189 except for AF, there must be other causes that the observed extreme strong inversion was not simulated
190 sufficiently by the model. This will be discussed in detail in the following sections.

191 3.3 The contributions to PM_{2.5} EG due to AF and DTD

192 Turbulent diffusion process is the main way of gas and particles exchanging from near ground to upper
193 atmosphere and then removed by the high altitude transport, which is usually described by turbulent
194 diffusion coefficient (DC) in the chemical atmospheric models. Firstly, the inversion and weak turbulent
195 diffusion, which generates from atmosphere dynamic process, leads to atmosphere stabilization and
196 determines the occurrence of haze and its strength (Zheng et al., 2017). Once the haze occurs, the aerosols
197 radiation may reinforce the inversion in turn when aerosols exceeds certain critical value and lead to more
198 PM_{2.5} gathering near the ground (Figure 4). The relative importance of the two aspects on PM_{2.5} EG may
199 vary with the PM_{2.5} values and meteorology conditions, but they are irreplaceable for the reasonable
200 prediction and simulation of PM_{2.5} peaks by atmospheric models.

201 Figure 5 displays the hourly changing of observed PM_{2.5} (PM_{2.5}_OBS) and modeled PM_{2.5} of Exp_bk,
202 EXP_td_af, and EXP_td20_tf experiments (PM_{2.5}_bk, PM_{2.5}_td_af, and PM_{2.5}_td20_af), together with the
203 modeled turbulent DC of the three experiments (DC_bk, DC_bk_af, and DC_td20_bf) from 15 to 23



204 December in Beijing (Figure 5a) and Xingtai (Figure 5b). Comparison of the $PM_{2.5_bk}$, $PM_{2.5_td_af}$, and
205 $PM_{2.5_td20_af}$ with $PM_{2.5_OBS}$ in Beijing (Figure 5a) shows that the modeled $PM_{2.5_td20_af}$ was the
206 closest to $PM_{2.5_OBS}$ during the whole haze episode, which was agreed with the results of regional
207 distribution during EGS in Figure 2. Exp_bk underestimated the $PM_{2.5}$ obviously from 17 to 22
208 December and this underestimation enlarged rapidly with the increasing of $PM_{2.5}$ values and the difference
209 between the modeled and observed $PM_{2.5}$ was the largest during the EGS of $PM_{2.5}$. AF shortened this
210 difference to a great extent and $PM_{2.5_td_af}$ was much closer to $PM_{2.5_OBS}$ than $PM_{2.5_bk}$ during $PM_{2.5}$
211 EGS. However, it can be seen that there was still certain differences between $PM_{2.5_OBS}$ and $PM_{2.5_td_af}$,
212 illustrating that AF can't completely fill the gap between $PM_{2.5_OBS}$ and $PM_{2.5_td_af}$. $PM_{2.5_td20_tf}$
213 shortened this gap further and shows the best agreement with the $PM_{2.5_OBS}$, especially during the EGS.

214 It also can be seen from figure 5a that the DC_bk was about 30-40 m^2/s during the EGS of $PM_{2.5}$,
215 which was about 50% of the 60-70 m^2/s on the clear day on 15 and 22 December. Obviously, the 50% DC
216 differences between the clear and haze days may be not enough to discriminate the difference of turbulent
217 diffusion intensity between extreme stable atmosphere on haze day and unstable atmosphere on clear day,
218 which may be the important reason for underestimation of $PM_{2.5}$ EG by Exp_bk . AF led to notable
219 enhancement of temperature inversion (Figure 4b), significant decrease in turbulent diffusion on $PM_{2.5}$
220 during EGS and DC_td_af was as low as 14 m^2/s on 20 December, which decreased about 50% comparing
221 with DC_bk . DC_td_af on haze day was only about 20% of that on clear day. The DC_td20_af was lower
222 than 5 m^2/s on 20 December and at the same time $PM_{2.5_td20_af}$ was further increased and it was also much
223 further closer to the $PM_{2.5_OBS}$ than $PM_{2.5_td_af}$.

224 It can be seen from the comparative study of the temporal changing between DC and $PM_{2.5}$ of Exp_bk ,
225 Exp_td_af , Exp_td20_af in Beijing that the overestimation of turbulent DC owing to lack of online
226 calculation of AF and deficient description of the extreme stable stratification by PBL schemes in
227 atmospheric model led to distinct underestimation of $PM_{2.5}$ EG and peaks when severe haze occurred in
228 Jing-Jin-Ji in China.

229 The changing trends of DC and $PM_{2.5}$ of the three sensitive experiments in Xingtai (Figure 5b) shows
230 the similar results with those in Beijing. The $PM_{2.5_td20_tf}$ was also the closest to $PM_{2.5_OBS}$, followed



231 by $PM_{2.5_td_af}$ and $PM_{2.5_bk}$ was the worst during the whole haze episode. However during the EGS of
232 $PM_{2.5}$, the relative contributions on the $PM_{2.5}$ peak values due to AF and DTD showed some difference with
233 those in Beijing. The contributions to $PM_{2.5}$ peaks due to DTD were more important than that by AF in
234 Xingtai. Located at the east foot of the east side of Taihang Mountains, Xingtai is usually affected by the
235 downhill airflow and temperature inversion in this area is easy to form and strengthened, leading to
236 stronger inversion, weaker turbulent diffusion and more stable atmospheric stratification. This kind of
237 inversion and weak turbulent diffusion derived from local terrain is more difficult to described and likely
238 underestimated by PBL scheme in atmospheric chemical models.

239 Figure 6 shows the diagrammatic sketch of the contributions to the $PM_{2.5}$ of EGS due to AF and DTD.
240 It can be seen that the DC_bk was $30\text{-}35\text{m}^2/\text{s}$, DC_td_af was $15\text{-}17\text{m}^2/\text{s}$, means that AF reduces about
241 43-57% DC based on EXP_bk , which led to the a rise in simulated $PM_{2.5}$ from 144 by EXP_bk to 205
242 $\mu\text{g}/\text{m}^3$ by EXP_td_af in Beijing, 280 by EXP_bk to 360 $\mu\text{g}/\text{m}^3$ EXP_td_af in Xingtai. This means that AF
243 reduced 20% in Beijing and 25% in Xingtai of simulated $PM_{2.5}$ negative errors. DC_td20_af was as low as
244 $4\text{-}6\text{m}^2/\text{s}$ during EGS of $PM_{2.5}$, showing the joint effects of AF and DTD reduced DC value to less than $4\text{-}6$
245 m^2/s , near-zero, we name it as “turbulent intermittent”. The direct results of this “turbulent intermittent” is
246 the further increasing of simulated $PM_{2.5}$ based on EXP_td_af . DTD decreases 14% to 20%
247 underestimation of simulated $PM_{2.5}$ and the errors of $PM_{2.5_td20_af}$ were reduced as low as -11% to 2%.

248 4 Conclusions

249 Using atmospheric chemical model GRAPES_CUACE, three experiments EXP_bk , EXP_td_af and
250 EXP_td20_af were designed to study the reason for the explosive growth of $PM_{2.5}$ mass during a red-alert
251 heavy haze occurred on 15 to 23 December, 2016 in JING-JIN-JI in China. The contributions to the $PM_{2.5}$
252 due to aerosols feedback and a further decrease in turbulent diffusion coefficient of chemical tracers,
253 representing a compensation for the deficient description of extreme weak turbulent diffusion by PBL
254 scheme in atmospheric models, are studied by analysing the changes of $PM_{2.5}$, temperature profiles,
255 diffusion coefficient and the relationship between them.

256 The study shows that the diffusion coefficient by EXP_bk is about $60\text{-}70\text{m}^2/\text{s}$ on clear day and
257 $30\text{-}35\text{m}^2/\text{s}$ on haze day. The 50% difference of the two was not considered enough to discriminate the



258 unstable atmosphere on clear day and extreme stable atmosphere on severe haze day, which is proved by
259 the weaker inversion calculated by EXP_bk than that of the actual sounding observation. This led to 40-51%
260 underestimation of the PM_{2.5} by EXP_bk during the explosive growth stage of PM_{2.5}. The surface daytime
261 cooling due to aerosols was 1.5-2.2 K during explosive growth stage of PM_{2.5} and 0.5-0.6 K during
262 climbing stage of PM_{2.5}. The impacts on PM_{2.5} due to AF was distinct during the explosive growth stage of
263 PM_{2.5} while very little during climbing stage of PM_{2.5} in the model run, indicating a critical value of 150
264 $\mu\text{g}/\text{m}^3$ of PM_{2.5} leading to an effective AF in online atmospheric chemical model. This aerosols' cooling
265 effect decreased rapidly with the height and this is the reason for the strengthening of the temperature
266 inversion during the explosive growth stage of PM_{2.5}. The local inversion by EXP_td_af was strengthened
267 and closer to the actual sounding observation than it by EXP_bk. This resulted in a 20-25% reduction of
268 PM_{2.5} underestimation and PM_{2.5} errors by EXP_td_af was as low as -16 to -11% during the explosive
269 growth stage of PM_{2.5}. However, the local inversion simulated by EXP_td_af was still weaker the actual
270 observation and the PM_{2.5}_td_af was still smaller than PM_{2.5} observation, illustrating that AF could not
271 solve all the PM_{2.5} underestimation problems. Further DTD of particles and gas resulted in another 14-20%
272 lessening of PM_{2.5} underestimation based on EXP_td_af and the PM_{2.5} errors of EXP_td20_af was reduced
273 to -11 to 2%.

274 This study result illustrated that the PBL scheme in current atmospheric chemical models is probably
275 insufficient for describing the extremely stable atmosphere resulting in explosive growth of PM_{2.5} and
276 severe haze in JING-JIN-JI in China, which may involve in two important reasons: One is the absence of
277 online calculation of AF, another is the deficient description of the extreme weak turbulent diffusion by
278 PBL scheme in the atmospheric chemical model. Our study suggests that online calculation of AF and an
279 improvement in arithmetic of turbulent diffusion in PBL schemes focusing on extreme stable atmosphere
280 stratification in atmospheric chemical model are indispensable for reasonable description of local
281 “turbulent intermittent” and accurate prediction the explosive growth and peaks of PM_{2.5} of severe haze in
282 Jing-Jin-Ji in China.

283

284



285

286 **Acknowledgements**

287 This study was supported by National Key Project of MOST. (JFYS2016ZY01002213), the National
288 Natural Science Foundation of China (41590874) and the National (Key) Basic Research and Development
289 (973) Program of China (2014CB441201)

290 **References**

- 291 Ding, A.J., Fu, C.B., Yang, X.Q., Sun, J.N., Petäjä, T., Kerminen, V.M., Wang, T., Xie, Y., Herrmann, E.,
292 Zheng, L.F., Nie, W., Liu, Q., Wei, X.L., Kulmala, M., 2013. Intense atmospheric pollution modifies
293 weather: a case of mixed biomass burning with fossil fuel combustion pollution in eastern China.
294 Atmos. Chem. Phys. 13 (20), 10545-10554.
- 295 Ding, A.J., Huang, X., Nie, W., Sun, J.N., Kerminen, V.M., Petäjä, T., Su, H., Cheng, Y.F., Yang, X.Q.,
296 Wang, M.H., Chi, X.G., Wang, J.P., Virkkula, A., Guo, W.D., Yuan, J., Wang, S.Y., Zhang, R.J., Wu,
297 Y.F., Song, Y., Zhu, T., Zilitinkevich, S., Kulmala, M., Fu, C.B., 2016. Enhanced haze pollution by
298 black carbon in megacities in China. Geophys. Res. Lett. 43 (6), 2873-2879.
- 299 Forkel, R., Werhahn, J., Hansen, A.B., McKeen, S., Peckham, S., Grell, G., Suppan, P., 2012. Effect of
300 aerosol-radiation feedback on regional air quality – A case study with WRF/Chem. Atmos. Environ. 53,
301 202-211.
- 302 Gao, M., Carmichael, G.R., Saide, P.E., Lu, Z., Yu, M., Streets, D.G., Wang, Z., 2016. Response of winter
303 fine particulate matter concentrations to emission and meteorology changes in North China. Atmos.
304 Chem. Phys. 16 (18), 11837-11851.
- 305 Gao, M., Saide, P.E., Xin, J., Wang, Y., Liu, Z., Wang, Y., Wang, Z., Pagowski, M., Guttikunda, S.K.,
306 Carmichael, G.R., 2017. Estimates of Health Impacts and Radiative Forcing in Winter Haze in Eastern
307 China through Constraints of Surface PM_{2.5} Predictions. Environ. Sci. Technol. 51 (4), 2178-2185.
- 308 Gao, Y., Zhao, C., Liu, X., Zhang, M., Leung, L.R., 2014. WRF-Chem simulations of aerosols and
309 anthropogenic aerosol radiative forcing in East Asia. Atmos. Environ. 92, 250-266.
- 310 Gao, Y., Zhang, M., Liu, Z., Wang, L., Wang, P., Xia, X., Tao, M., Zhu, L., 2015. Modeling the feedback
311 between aerosol and meteorological variables in the atmospheric boundary layer during a severe fog–



- 312 haze event over the North China Plain. Atmos. Chem. Phys. 15 (8), 4279-4295.
- 313 Gong, S.L., Zhang, X.Y., 2007. CUACE/Dust – an integrated system of observation and modeling systems
314 for operational dust forecasting in Asia. Atmos. Chem. Phys. Discuss. 7 (4), 1061-1067.
- 315 Hong, S.Y., Noh, Y., Dudhia, J., 2006. A New Vertical Diffusion Package with an Explicit Treatment of
316 Entrainment Processes. Mon. Weather Rev. 134 (9), 2318-2341.
- 317 Hu, X.M., Doughty, D.C., Sanchez, K.J., Joseph, E., Fuentes, J.D., 2012. Ozone variability in the
318 atmospheric boundary layer in Maryland and its implications for vertical transport model. Atmos.
319 Environ. 46, 354-364.
- 320 Hu, X.M., Klein, P.M., Xue, M., 2013. Evaluation of the updated YSU planetary boundary layer scheme
321 within WRF for wind resource and air quality assessments. J. Geophys. Res. Atmos. 118 (18),
322 10490-10505.
- 323 Hu, X.M., Klein, P.M., Xue, M., Zhang, F., Doughty, D.C., Forkel, R., Joseph, E., Fuentes, J.D., 2013.
324 Impact of the vertical mixing induced by low-level jets on boundary layer ozone concentration. Atmos.
325 Environ. 70, 123-130.
- 326 Hua, Y., Wang, S., Wang, J., Jiang, J., Zhang, T., Song, Y., Kang, L., Zhou, W., Cai, R., Wu, D., Fan, S.,
327 Wang, T., Tang, X., Wei, Q., Sun, F., Xiao, Z., 2016. Investigating the impact of regional transport on
328 PM_{2.5} formation using vertical observation during APEC 2014 Summit in Beijing. Atmos. Chem.
329 Phys. 16, 15451–15460.
- 330 Huang, R.J., Zhang, Y., Bozzetti, C., Ho, K.F., Cao, J.J., Han, Y., Daellenbach, K.R., Slowik, J.G., Platt,
331 S.M., Canonaco, F., Zotter, P., Wolf, R., Pieber, S.M., Bruns, E.A., Crippa, M., Ciarelli, G.,
332 Piazzalunga, A., Schwikowski, M., Abbaszade, G., Schnelle-Kreis, J., Zimmermann, R., An, Z., Szidat,
333 S., Baltensperger, U., El Haddad, I., Prevot, A.S., 2014. High secondary aerosol contribution to
334 particulate pollution during haze events in China. Nature. 514 (7521), 218-222.
- 335 Jiang, C., Wang, H., Zhao, T., Li, T., Che, H., 2015. Modeling study of PM_{2.5} pollutant transport across
336 cities in China's Jing–Jin–Ji region during a severe haze episode in December 2013. Atmos. Chem.
337 Phys. 15 (10), 5803-5814.
- 338 Li, K., Liao, H., Zhu, J., Moch, J.M., 2016. Implications of RCP emissions on future PM_{2.5} air quality and



- 339 direct radiative forcing over China. *J. Geophys. Res. Atmos.* 121 (21), 12985-13008.
- 340 Li, T., Wang, H., Zhao, T., Xue, M., Wang, Y., Che, H., Jiang, C., 2016. The Impacts of Different PBL
341 Schemes on the Simulation of PM_{2.5} during Severe Haze Episodes in the Jing-Jin-Ji Region and Its
342 Surroundings in China. *Adv. Meteorol.* 2016, 1-15.
- 343 Miao, Y., Liu, S., Zheng, Y., Wang, S., 2016. Modeling the feedback between aerosol and boundary layer
344 processes: a case study in Beijing, China. *Environ. Sci. Pollut R.* 23 (4), 3342-3357.
- 345 Petäjä, T., Järvi, L., Kerminen, V.M., Ding, A.J., Sun, J.N., Nie, W., Kujansuu, J., Virkkula, A., Yang, X.Q.,
346 Fu, C.B., Zilitinkevich, S., Kulmala, M., 2016. Enhanced air pollution via aerosol-boundary layer
347 feedback in China. *Sci. Rep.* 6, 18998.
- 348 Qiu, Y., Liao, H., Zhang, R., Hu, J., 2017. Simulated impacts of direct radiative effects of scattering and
349 absorbing aerosols on surface layer aerosol concentrations in China during a heavily polluted event in
350 February 2014. *J. Geophys. Res. Atmos.* 122 (11), 5955-5975.
- 351 Quan, J., Tie, X., Zhang, Q., Liu, Q., Li, X., Gao, Y., Zhao, D., 2014. Characteristics of heavy aerosol
352 pollution during the 2012–2013 winter in Beijing, China. *Atmos. Environ.* 88, 83-89.
- 353 Sun, Y., Jiang, Q., Wang, Z., Fu, P., Li, J., Yang, T., Yin, Y., 2014. Investigation of the sources and evolution
354 processes of severe haze pollution in Beijing in January 2013. *J. Geophys. Res. Atmos.* 119 (7),
355 4380-4398.
- 356 Wang, H., Gong, S., Zhang, H., Chen, Y., Shen, X., Chen, D., Xue, J., Shen, Y., Wu, X., Jin, Z., 2009. A
357 new-generation sand and dust storm forecasting system GRAPES_CUACE/Dust: Model development,
358 verification and numerical simulation. *Chinese Sci. Bull.* 55 (7), 635-649.
- 359 Wang, H., Zhang, X., Gong, S., Chen, Y., Shi, G., Li, W., 2010. Radiative feedback of dust aerosols on the
360 East Asian dust storms. *J. Geophys. Res.* 115 , D23214.
- 361 Wang, H., Tan, S.C., Wang, Y., Jiang, C., Shi, G.Y., Zhang, M.X., Che, H.Z., 2014a. A multi sources
362 observation study of the severe prolonged regional haze episode over eastern China in January 2013.
363 *Atmos. Environ.* 89, 807-815.
- 364 Wang, H., Xu, J., Zhang, M., Yang, Y., Shen, X., Wang, Y., Chen, D., Guo, J., 2014b. A study of the
365 meteorological causes of a prolonged and severe haze episode in January 2013 over central-eastern



- 366 China. Atmos. Environ. 98, 146-157.
- 367 Wang, H., Xue, M., Zhang, X.Y., Liu, H.L., Zhou, C.H., Tan, S.C., Che, H.Z., Chen, B., Li, T., 2015a.
- 368 Mesoscale modeling study of the interactions between aerosols and PBL meteorology during a haze
- 369 episode in Jing-Jin-Ji (China) and its nearby surrounding region – Part 1: Aerosol distributions and
- 370 meteorological features. Atmos. Chem. Phys. 15 (6), 3257-3275.
- 371 Wang, H., Shi, G.Y., Zhang, X.Y., Gong, S.L., Tan, S.C., Chen, B., Che, H.Z., Li, T., 2015b. Mesoscale
- 372 modelling study of the interactions between aerosols and PBL meteorology during a haze episode in
- 373 China Jing-Jin-Ji and its near surrounding region - Part 2: Aerosols' radiative feedback effects. Atmos.
- 374 Chem. Phys. 15 (6), 3277-3287.
- 375 Wang, J., Wang, S., Jiang, J., Ding, A., Zheng, M., Zhao, B., Wong, D.C., Zhou, W., Zheng, G., Wang, L.,
- 376 Pleim, J.E., Hao, J., 2014. Impact of aerosol-meteorology interactions on fine particle pollution during
- 377 China's severe haze episode in January 2013. Environ. Res. Lett. 9 (9), 094002.
- 378 Wang, Y., Zhang, Q.Q., He, K., Zhang, Q., Chai, L., 2013. Sulfate-nitrate-ammonium aerosols over China:
- 379 response to 2000–2015 emission changes of sulfur dioxide, nitrogen oxides, and ammonia. Atmos.
- 380 Chem. Phys. 13 (5), 2635-2652.
- 381 Wang, Z., Li, J., Wang, Z., Yang, W., Tang, X., Ge, B., Yan, P., Zhu, L., Chen, X., Chen, H., Wand, W., Li,
- 382 J., Liu, B., Wang, X., Wand, W., Zhao, Y., Lu, N., Su, D., 2013. Modeling study of regional severe
- 383 hazes over mid-eastern China in January 2013 and its implications on pollution prevention and control.
- 384 Sci. China Earth Sci. 57 (1), 3-13.
- 385 Yang, Y., Liao, H., Lou, S., 2016. Increase in winter haze over eastern China in recent decades: Roles of
- 386 variations in meteorological parameters and anthropogenic emissions. J. Geophys. Res. Atmos. 121
- 387 (21), 13050-13065.
- 388 Yang, Y.R., Liu, X.G., Qu, Y., An, J.L., Jiang, R., Zhang, Y.H., Sun, Y.L., Wu, Z.J., Zhang, F., Xu, W.Q., Ma,
- 389 Q.X., 2015. Characteristics and formation mechanism of continuous hazes in China: a case study
- 390 during the autumn of 2014 in the North China Plain. Atmos. Chem. Phys. 15 (14), 8165-8178.
- 391 Zhang, M., H. Wang, X. Y. Zhang, et al., 2018. Applying the WRF double-moment six-class microphysics
- 392 scheme in the GRAPES_Meso model: A case study. J. Meteor. Res., 32(2), 246–264, doi:



- 393 10.1007/s13351018-7066-1.
- 394 Zhang, R.H., Li, Q., Zhang, R., 2013. Meteorological conditions for the persistent severe fog and haze
395 event over eastern China in January 2013. *Sci. China Earth Sci.* 57 (1), 26-35.
- 396 Zheng, G., Duan, F., Ma, Y., Zhang, Q., Huang, T., Kimoto, T., Cheng, Y., Su, H., He, K., 2016.
397 Episode-Based Evolution Pattern Analysis of Haze Pollution: Method Development and Results from
398 Beijing, China. *Environ. Sci. Technol.* 50 (9), 4632-4641.
- 399 Zheng, G.J., Duan, F.K., Su, H., Ma, Y.L., Cheng, Y., Zheng, B., Zhang, Q., Huang, T., Kimoto, T., Chang,
400 D., Pöschl, U., Cheng, Y.F., He, K.B., 2015. Exploring the severe winter haze in Beijing: the impact of
401 synoptic weather, regional transport and heterogeneous reactions. *Atmos. Chem. Phys.* 15 (6),
402 2969-2983.
- 403 Zhong, J., Zhang, X., Wang, Y., Sun, J., Zhang, Y., Wang, J., Tan, K., Shen, X., Che, H., Zhang, L., Zhang,
404 Z., Qi, X., Zhao, H., Ren, S., Li, Y., 2017. Relative contributions of boundary-layer meteorological
405 factors to the explosive growth of PM_{2.5} during the red-alert heavy pollution episodes in Beijing in
406 December 2016. *J. Meteorol. Res.* 31 (5), 809-819.
- 407 Zhong, J.T., Zhang, X.Y., Dong, Y.S., Wang, Y.Q., Liu, C., Wang, J.Z., Zhang, Y.M., Che, H.C., 2018.
408 Feedback effects of boundary-layer meteorological factors on cumulative explosive growth of PM_{2.5}
409 during winter heavy pollution episodes in Beijing from 2013 to 2016. *Atmos. Chem. Phys.* 18, 247–
410 258.
- 411 Zhou, C.H., Gong, S., Zhang, X.Y., Liu, H.L., Xue, M., Cao, G.L., An, X.Q., Che, H.Z., Zhang, Y.M., Niu,
412 T., 2012. Towards the improvements of simulating the chemical and optical properties of Chinese
413 aerosols using an online coupled model – CUACE/Aero. *Tellus B.* 64 (1), 91-102.
- 414 Zhou, C., Zhang, X., Gong, S., Wang, Y., Xue, M., 2016. Improving aerosol interaction with clouds and
415 precipitation in a regional chemical weather modeling system. *Atmos. Chem. Phys.* 16 (1), 145-160.
416



417

418

419

420

Table 1 Experiments Design

EXP_bk	Background model experiment: ignoring aerosol radiation feedback, normal turbulent diffusion of chemical tracers
EXP_td_af	Model run with aerosols radiation feedback online, normal turbulent diffusion of chemical tracers
EXP_td20_af	Model run with aerosols radiation feedback online, retaining 20% (reducing 80%) of normal turbulent diffusion of chemical tracers, representing a supposed compensation for the deficient description of extreme weak turbulent diffusion by PBL scheme

421

422

423



424

425

426

Figure

427 **Fig.1** Model domain (a), cities locations and the topography features in Jing-Jin-Ji (b)

428 **Fig.2** Observed $PM_{2.5}$ (OBS_ $PM_{2.5}$) and simulated $PM_{2.5}$ ($\mu\text{g}/\text{m}^3$) of EGS by Exp_bk ($PM_{2.5_bk}$)

429 EXP_td_af ($PM_{2.5_td_af}$), and EXP_td20_tf ($PM_{2.5_td20_af}$).

430 **Fig.3** Variation of temperature profiles due to aerosol radiation (K) from 15 to 20 December, 2016.

431 **Fig.4** Sounding observed and modeled temperature profiles by EXP_bk and EXP_af_td during CS (a) and

432 EGS (b) in Beijing and Xingtai.

433 **Fig.5** Hourly changing of $PM_{2.5_OBS}$, $PM_{2.5_bk}$, $PM_{2.5_td_af}$, and $PM_{2.5_td20_tf}$ ($\mu\text{g}/\text{m}^3$), together with

434 the turbulent diffusion coefficient (DC_bk, DC_td_af, and DC_td20_af) of the three experiments from 15

435 to 22 December, 2016 in Beijing (a) and Xingtai (b)

436 **Fig.6** The diagrammatic sketch of the contributions to the $PM_{2.5}$ EG due to ARF and DTD

437

438

439

440

441

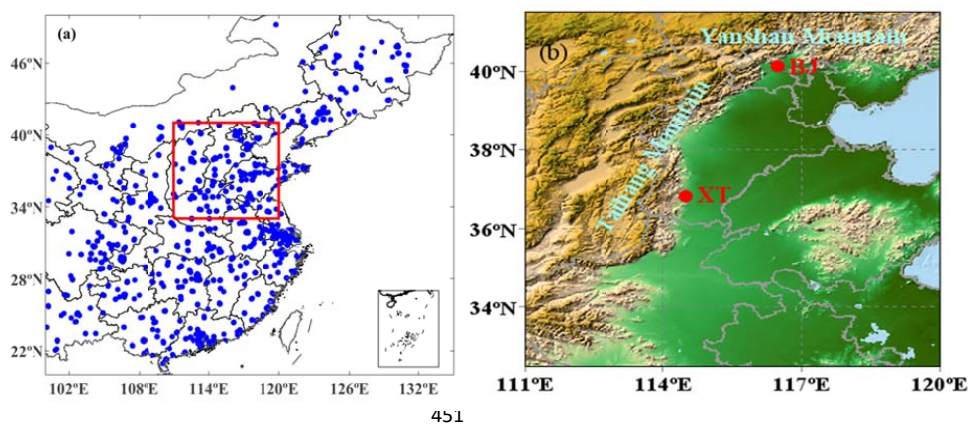
442

443

444



446



448 Fig. 1 Model domain (a), cities locations and the topography features in Jing-Jin-Ji (b)

449

450

451

452

453

454

455

456

457

458

459

460

461

462

463

464

465

466

467

468

469

470

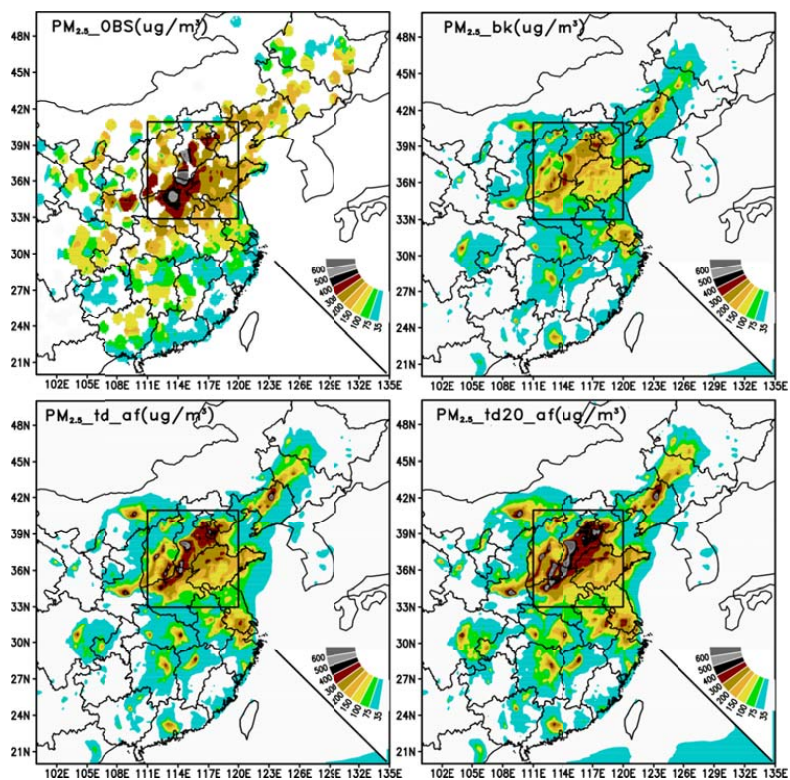
471

472

473



474
475
476
477
478
479
480
481
482
483
484
485
486
487
488
489
490
491
492
493
494
495
496
497



499 **Fig.2** Observed $PM_{2.5}$ (OBS_ $PM_{2.5}$) and simulated $PM_{2.5}$ ($\mu\text{g}/\text{m}^3$) of EGS by Exp_bk ($PM_{2.5_bk}$)
500 EXP_td_af ($PM_{2.5_td_af}$), and EXP_td20_tf ($PM_{2.5_td20_af}$).

501
502
503



504
505
506
507
508
509
510
511
512
513
514
515
516
517
518
519
520
521
522
523
524
525
526
527
528
529
530
531
532
533
534
535
536
537
538
539
540
541
542
543
544

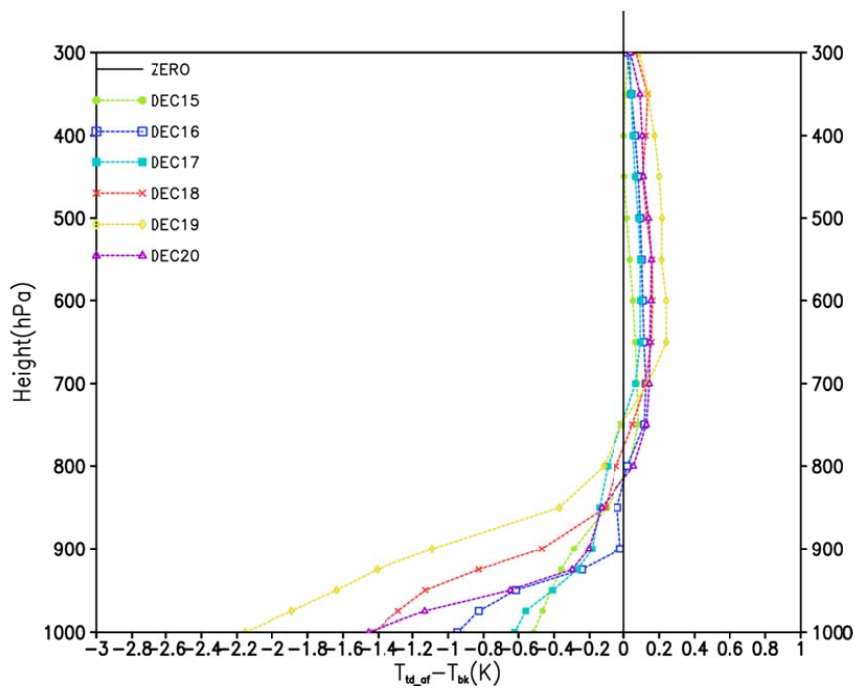
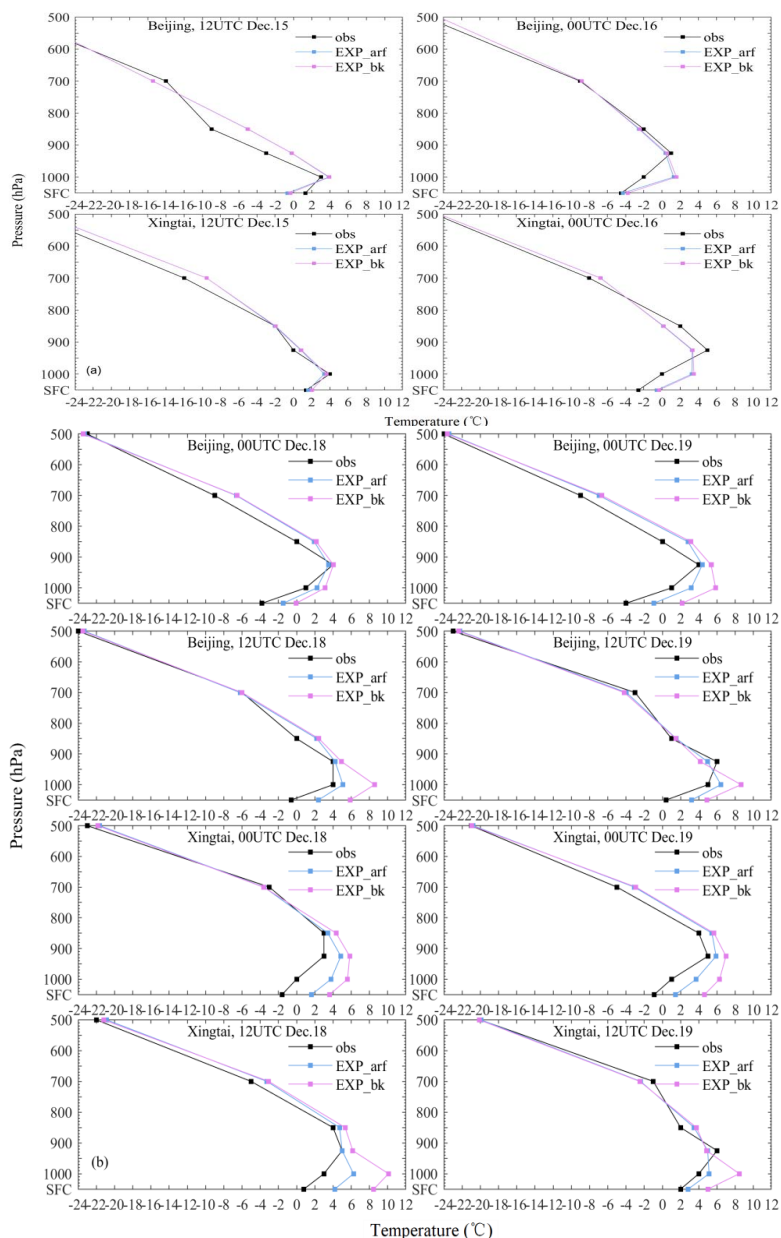


Fig. 3 Variation of temperature profiles by aerosol radiation (K) from 15 to 20 December, 2016.



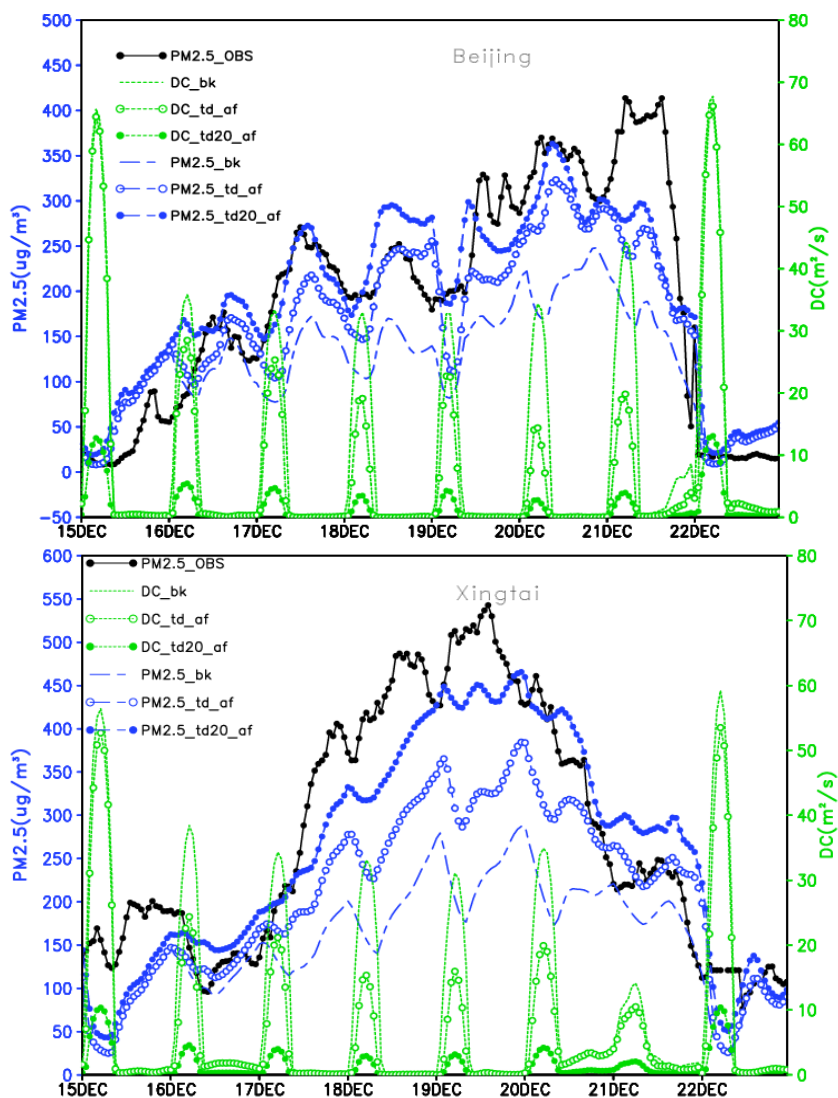
544
545
546
547
548
549
550
551
552
553
554
555
556
557
558
559
560
561
562
563
564
565
566
567
568
569
570
571
572
573
574
575
576
577



578 **Fig.4** Sounding observed and modeled temperature profiles by EXP_bk and EXP_af_td during CS (a) and
579 EGS (b) in Beijing and Xingtai.



580



581

582 **Fig.5** Hourly changing of Observed and modeled $PM_{2.5}$ ($\mu g/m^3$) of Exp_bk, EXP_td_af, and
 583 EXP_td20_tf, together with the turbulent diffusion coefficient (DC) of the three experiments from 15 to
 584 22 December, 2016 in Beijing (a) and Xingtai (b)

585

586

587



588
 589
 590
 591
 592
 593
 594
 595
 596
 597
 598
 599
 600
 601
 602
 603
 604
 605
 606
 607
 608
 609
 610
 611
 612
 613
 614
 615
 616
 617
 618
 619
 620
 621
 622
 623
 624
 625
 626
 627

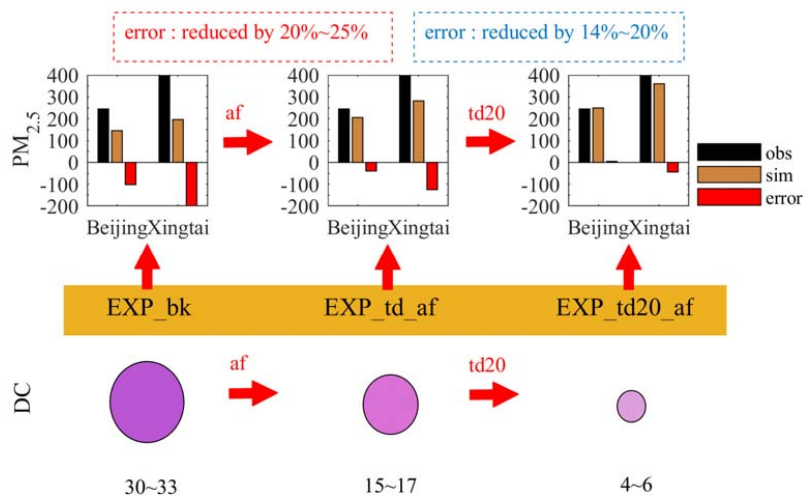


Fig.6 The diagrammatic sketch of the contributions to the PM_{2.5} EG due to AF and DTD